

A Comparison Between Conventional and Collapse-Mode Capacitive Micromachined Ultrasonic Transducers in 10-MHz 1-D Arrays

Kwan Kyu Park, *Member, IEEE*, Ömer Oralkan, *Senior Member, IEEE*,
and Butrus T. Khuri-Yakub, *Fellow, IEEE*

Abstract—This paper presents a comprehensive comparison between a collapse-mode and a conventional-mode capacitive micromachined ultrasonic transducer (CMUT); both devices have a 1- μm -thick silicon plate and operate at 10 MHz when biased at 100 V. The radii of the circular plates and the gap heights are modified to meet the design specifications required for a fair comparison. Finite element analysis (FEA) shows that the collapse-mode CMUT has higher output pressure sensitivity (46.5 kPa/V) than the conventional CMUT (13.1 kPa/V), and achieves a 3-dB fractional bandwidth (FBW) of 124% compared with 128% for the conventional mode. These results were validated by experiments performed on devices fabricated in a 1-D phased array configuration using the local oxidation of silicon (LOCOS)/wafer-bonding process. The measured output pressure sensitivity and the FBW of the collapse-mode and the conventional CMUTs at 100 V were 26.4 kPa/V and 103% and 12.7 kPa/V and 111%, respectively. The maximum output pressure of the collapse-mode CMUT was 1.19 MPa at 10 MHz, which was much higher than the conventional CMUT (0.44 MPa). However, the second harmonic distortion (SHD) level of the collapse-mode CMUT is higher than the conventional CMUT at the same excitation condition. Even with higher electric field in the cavity, the collapse-mode CMUT was as stable as the conventional CMUT in a long-term test. A 30-h test with a total of 3.2×10^9 cycles of 30 V ac excitation resulted in no significant degradation in the performance of the collapse-mode devices.

I. INTRODUCTION

CAPACITIVE micromachined ultrasonic transducers (CMUTs) have been investigated as an alternative to piezoelectric ultrasound transducers. Compared with piezoelectric transducers, which generate sound by a bulk acoustic wave, the CMUTs utilize the flexural mode of thin plates to generate or to receive sound. Because of the low mechanical impedance of the thin plate, the mechanical matching of the CMUTs to the fluid medium is

better than that of piezoelectric transducers. As a result, CMUTs have wider fractional bandwidth than piezoelectric transducers and do not require matching layers. In addition to the advantages in acoustic properties, CMUTs have more design flexibility. CMUTs leverage well-established microfabrication techniques, e.g., photolithography, to implement transducer arrays with complex configurations. For example, a 4-MHz 64-element 1-D transducer [1], a 4.38-MHz 128×128 element 2-D transducer [2], and a 64-element ring array [3] have been presented previously. An additional benefit of using silicon microfabrication techniques is the flexibility in the integration of these complex transducer arrays with supporting front-end electronic circuits [4].

To utilize these benefits in various applications, the output pressure of the CMUTs must be in the 1 to 3 MPa range. In ultrasound imaging applications, a transducer capable of transmitting high output pressure up to the FDA regulated limits is preferred to obtain the maximum possible SNR and depth of penetration. Therapeutic high-intensity focused ultrasound (HIFU) is another example of the demand for high output pressure. To meet these demands, extensive research has focused on improving the output pressure of the CMUT without reducing the bandwidth. One approach is using the CMUT in an unconventional operation mode in which the plate is partially in contact with the substrate at all times. By applying a dc bias voltage greater than the pull-in voltage, the center of a plate comes in contact with the substrate (collapsed). In this operation, the center of the plate is supported by the substrate and the rim of the plate is clamped. Therefore, only a doughnut-shaped area acts as the moving plate structure. This mode of operation is referred to as collapse-mode.

Fig. 1 presents the static deflection of the CMUT in both the conventional mode and the collapse-mode. There are two clear benefits in the collapse-mode operation of the CMUT. First, a cell (a unit transducer) has higher electric field sustained through the cavity compared the conventional mode. This increased electric field is caused by two factors: higher bias voltage and lower effective gap height. The increase of the electric field overcomes the possible loss of performance resulting from the parasitic capacitance of the now-collapsed area [5], [6]. As a result, the collapse-mode presents better performance in both transmit (TX) and receive (RX) sensitivities. Second, the cell in the collapse-mode has a higher ratio of average dis-

Manuscript received May 18, 2012; accepted March 7, 2013. This work was supported by the National Institute of Health under Grants HL67647 and CA134720. This work was performed, in part, at the Stanford Nanofabrication Facility (a member of the National Nanotechnology Infrastructure Network), which is supported by the National Science Foundation under Grant ECS-9731293.

K. K. Park and B. T. Khuri-Yakub are with the Edward L. Ginzton Laboratory, Stanford University, Stanford, CA (e-mail: kwankyup@stanford.edu).

Ö. Oralkan was with the Edward L. Ginzton Laboratory, Stanford University, Stanford, CA. He is now with the Department of Electrical and Computer Engineering, North Carolina State University, Raleigh, NC.

DOI <http://dx.doi.org/10.1109/TUFFC.2013.2688>

placement (u_{avg}) to peak displacement (u_{max}). When the bias voltage changes from 50 V to 60 V, the center of the plate ($X = 0 \mu\text{m}$) moves by 37.0 nm (u_{max}), whereas the average displacement (u_{avg}), i.e., the change of average deflection is 11.8 nm. That means the ratio between the u_{avg} and u_{max} is 0.32 for the conventional mode. In the case of the collapse-mode CMUT, when the bias voltage changes from 75 V to 85 V, the ratio ($u_{\text{avg}}/u_{\text{max}}$) increases to 0.44. The peak displacement (u_{max}) of the CMUT is limited to the gap height. Therefore, the collapse-mode transducer has a greater upper limit of volume displacement, i.e., more output pressure.

There have been several experimental and theoretical investigations on the collapse-mode operation of CMUTs. Oralkan *et al.* [5] and Huang *et al.* [6] experimentally investigated the behavior of the collapse-mode CMUTs. The experimental results show the benefit of the collapse-mode CMUT in terms of transmit and receive sensitivities with a wide fractional bandwidth [5]. However, the previous work [5]–[7] operated the same CMUTs in both conventional and collapse mode by applying different bias voltages. Therefore, the comparison between the conventional and the collapse mode was based on two conditions of the CMUT, at which the devices had different center frequencies and operating bias voltages. To compare these two modes in the same operating conditions, various designs of collapse-mode CMUTs have been simulated using FEA [8], [9] and using analytical methods [10].

In this paper, we present a comprehensive comparison between a collapse-mode CMUT and a conventional-mode CMUT. The significance of this study is that we experimentally compare two devices of the same center frequency and the same operating dc bias voltage. To compare

them in a realistic case, we designed both devices in a 1-D phased array configuration, in which the width of the element is smaller than half a wavelength in water at the center frequency. The two devices are compared experimentally in terms of output pressure, frequency response, second harmonic distortion, and long-term stability. These experimental results are also used to validate the finite-element models. The organization of this paper is as follows. Section II briefly describes the two designs used in this study. The FEA results based on these designs are presented in Section III. The device fabrication is summarized in Section IV and the measurement results of the fabricated devices are presented in Section V.

II. DEVICE DESIGN

For a comparison between the conventional CMUT and the collapse-mode CMUT, these devices should have the same operating parameters. The first parameter is the center frequency. When the plate is pulled in, the center frequency typically increases by a factor of 2 to 3 in immersion. Thus, the plate of the collapse-mode CMUT should have much lower fundamental frequency (i.e., the center frequency before the pull-in condition) than the conventional CMUT. To meet this criterion, the plate of the collapse-mode CMUT should be larger in radius or thinner than the conventional CMUTs. Second, both devices should have the same element-to-element pitch. In this paper, we present a 1-D phased array configuration with an element-to-element pitch of half the wavelength at the frequency of interest. Third, these devices should have similar operating bias voltage; the pull-in voltage of the conventional CMUT should be higher than the operating voltage, whereas that of the collapse-mode CMUT should be lower than the operating voltage. For comparison, we selected the center frequency as 10 MHz and a corresponding element-to-element pitch of 75 μm . We also choose the operating bias voltage to be around 100 V.

In the design step, the fabrication feasibility should be considered as well. The upper and lower limits of key dimensions, such as the plate thickness and radius, and the material of the device are decided by the fabrication technology to be used. In this paper, we choose the CMUT fabrication technology based on a local oxidation of silicon (LOCOS)-wafer/bonding process [11]. Based on the fabrication process, the plate is made of single-crystal silicon and the possible thickness of the plate ranges from sub-micrometer to hundreds of micrometers. For comparison, we chose the thickness of the plate to be 1 μm , which is a typical value in CMUT design for ultrasound imaging applications. Based on the previously listed criteria, we selected the key dimensions of the two devices as shown in Table I. To decrease the fundamental frequency of the collapse-mode CMUT, we chose to increase the radius of the cell to 30 μm . Because the element-to-element pitch is 75 μm , one element of the conventional-mode CMUT is made of two columns of cells, whereas the element of the

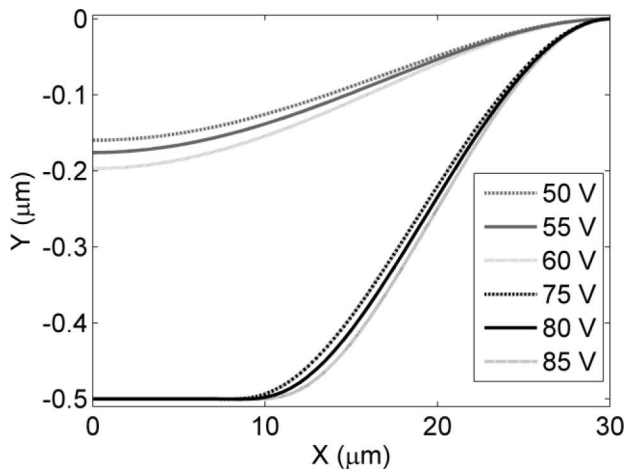


Fig. 1. Static deflection of circular silicon plate in the conventional and the collapse modes (radius: 30 μm , thickness: 1 μm). At bias voltages ranging from 50 to 60 V, the average displacement, i.e., the change of average static deflection, is 11.8 nm and the maximum displacement is 37.0 nm (at $X = 0 \mu\text{m}$). In the collapse mode, at bias voltages ranging from 75 to 85 V, the average displacement is 16.0 nm and the maximum displacement is 35.9 nm (at $X = 16.5 \mu\text{m}$). For the collapse mode, the calculation of the average displacement takes the contact area ($X < 10 \mu\text{m}$) into account.

collapse-mode CMUTs is made of a single column of cells. As a result, both devices have the same fill factor of the cell, which is 50%. The gap heights of both designs were selected to have the same operating bias voltage, around 100 V, which is 74% and 141% of the pull-in voltages of the conventional-mode CMUT and the collapse-mode CMUT, respectively.

III. FINITE ELEMENT ANALYSIS

The two designs described in the previous section were analyzed using a finite element analysis (FEA) model¹ developed in ANSYS (ver. 13, ANSYS Inc., Canonsburg, PA). The analysis was performed in two parts. First, the output pressure response was calculated in 2-D axisymmetric harmonic analysis. Based on this analysis, the center frequency, the output pressure, and the fractional bandwidth can be estimated. The 2-D analysis was also used in the design step to estimate the pull-in voltage and the center frequency. Second, the dynamic response was calculated using a 3-D analysis, in which the model simulates the phased array configuration and mainly focuses on the frequency response based on the large-signal pulsed excitation.

A. 2-D FEA Model

The single cell of the CMUT is modeled in 2-D axisymmetric coordinates; the model includes a circular plate and a cylindrically shaped fluid column on the plate. The fluid column (FLUID29) covers the top of the plate (PLANE42) to include the effect of the acoustic loading. A protective layer or matching layer is not used. To simulate the CMUT plates in a periodic distribution in the 2-D axisymmetric model, the outer radius of the fluid column is chosen so that the 2-D model and an actual device have the same ratio between the plate and non-active areas [12]. The typical mesh size of the plate is 0.25 μm and the plate has 4 elements along the thickness. An electrostatic force is applied on the bottom of the plate by electro-mechanical transducer elements (TRANS126), which are attached to all nodes on the bottom of the plate. The TRANS126 elements also act as contact elements; by setting the minimum gap height of the TRANS126 elements to be the effective thickness of dielectric layer inside the CMUT cell, the TRANS126 elements behave like contact elements in the collapse mode. The contact stiffness (KN) of the TRANS126 element should be maximized to simulate the stiff insulation layers as long as the FEA converges into a solution.

In the collapse-mode operation, the amount of deflection is not negligible compared with the plate thickness.

¹In both 2-D and 3-D models, we used the following properties. The Young's modulus of the plate: 148 GPa. The Poisson's ratio of the plate: 0.1773. The density of the plate: 2329 kg/m³. The thickness of the insulation layer: 110 nm. The relative permittivity of the insulation layer: 3.7.

TABLE I. DIMENSIONS OF THE CONVENTIONAL CMUT AND THE COLLAPSE-MODE CMUT.

	Conventional CMUT	Collapse-mode CMUT
Plate thickness (μm)	1	1
Cell radius (μm)	15	30
Cell-to-cell pitch (μm)	33	65
Gap (μm)	0.25	0.5
$V_{\text{pull-in}}$ (V), FEA	135	71

In this case, the deflection increases the tensile stress of the plate and can affect the effective stress of the plate. To include these factors in the FEA, large deflection effects (NLGEOM, ON) and stress stiffening effects (SSTIF, ON) are enabled in the pre-stress (static) analysis.²

A sound wave from the plate, which is excited by the electrostatic force, propagates through the fluid column, and is absorbed by an absorbing boundary on top of the column. In the calculation, first the static analysis is performed including the electrostatic force and the atmospheric pressure. The result from the static analysis serves as the initial condition of the harmonic analysis. In the harmonic analysis, ac excitation voltage, which does not have source impedance, is applied on dc bias; the pressure information at each excitation frequency is extracted from every node, which is located at the interface between the medium and the plate. The average pressure is calculated from the pressure distribution across the plate and the space between the plates. A detailed description of the 2-D FEA model is presented in [12].

The two CMUTs described in Table I were biased at 100 V dc and the output pressure for each transducer was calculated as shown in Fig. 2 and Table II. At 100 V, the collapsed device has 3.5 times higher output pressure, while demonstrating similar peak frequency. In addition, the collapse-mode CMUT has broader fractional bandwidth (FBW) than the conventional CMUT, which agrees with the previous experimental work on collapse-mode operation [6]. The output pressure is a strong function of the dc bias voltage. Therefore, we calculated the output pressure in various bias voltages using the described models. The CMUTs were biased at voltages ranging from 10 to 180 V, and the output pressure at 10 MHz was calculated as shown in Fig. 3. The conventional mode CMUT and the collapse-mode CMUT showed a rapid increase in the output pressure at 140 V and 80 V, respectively; the increase was due to the pull-in of the plate. The calculated pull-in voltages of the conventional and collapse-mode devices are 135 V and 71 V, respectively. In the range of 80 to 130 V dc bias, the collapse-mode CMUT has 1.7 to 3.5 times higher output pressure than the conventional mode CMUT when biased at the same dc voltage.

²For a check of assumptions, the static analysis and the transient analysis were performed additionally on the collapse-mode CMUT. In the case of the collapse-mode CMUT in Table I, the effects of the large deflection and the stress stiffening are observed and found to be negligible.

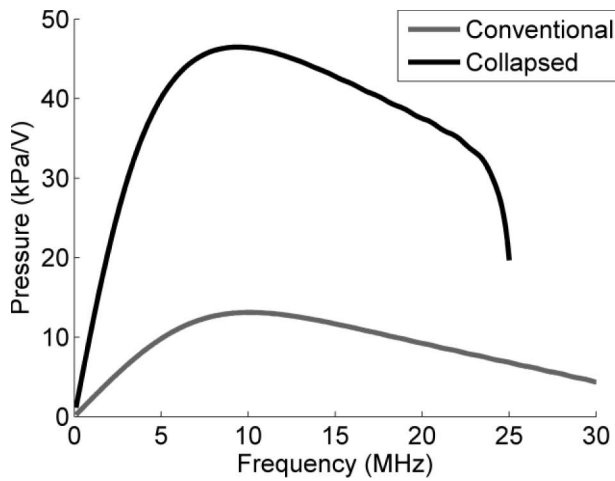


Fig. 2. Output pressure sensitivities calculated from the harmonic analysis of 2-D FEA models in Table I.

The 2-D FEA model has several benefits; its short computation time is useful in the initial design stage for fast iteration. It also supplies accurate results for large elements in the CW mode. However, the 2-D model assumes that the element is made of an infinite number of cells. This assumption may not be valid in the 1-D phased array configuration, in which the width of an element is smaller than the wavelength. To simulate the 1-D array configuration, a 3-D FEA model was developed to predict the frequency response of the actual fabricated devices.

B. 3-D FEA Model

The purpose of the 3-D finite element (FE) model is to simulate the actual configurations of the described CMUTs, a 1-D phased array was developed in an FE model as depicted in Fig. 4(a). Because of the large number nodes in the 3-D FE model, it is impractical to calculate the response of that many cells including the medium on top. Therefore, the model was simplified based on following assumptions: 1) the 1-D array has an infinite length, and 2) all cells in each element have identical responses. Based on these assumptions, a cell can represent a column of cells; the example is shown in Fig. 4(a). By modeling the 14 gray cells and the medium on the cells, the response of an infinite-length semi-cylinder model can be calculated. To realize the assumptions, the degrees of freedom (DOFs) of all nodes of one semicircle in the medium were coupled to the DOFs of corresponding nodes on another semicircle. As shown in Fig. 4(a), the active element,

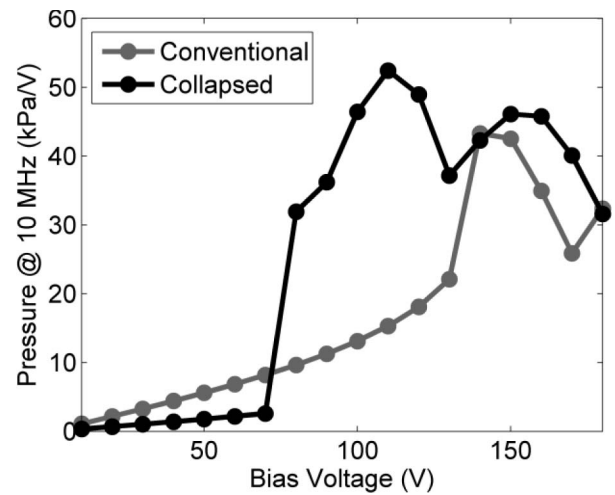


Fig. 3. Output pressure sensitivities at 10 MHz at various dc bias voltages. The results were calculated from the harmonic analysis of 2-D FEA models described in Table I.

i.e., excited element, of the conventional CMUT has two columns of cells, whereas the collapse-mode CMUT has an active element made of a single column of cells. Other neighboring cells act as the adjacent elements in the actual device.

The 3-D FE model is developed in ANSYS. The approach is similar to the 2-D modeling, but requires several modifications; the plate is made of SOLID187 elements and the fluid on top is made of FLUID30 and FLUID130 elements. Because of the heavy computation time of the 3-D model, the mesh size should be optimized. The plate has 10 meshes along the radius and 4 meshes along the thickness. The mesh size of the medium is 1/10 of the wavelength in the frequency of interest. After defining and meshing the plates and the medium, the electromechanical transducer elements (TRANS126) are attached to all nodes at the bottom of the plates. To simulate the collapse mode, the minimum gap height and the contact stiffness (KN) of TRANS126 elements are defined as described in the previous section. For the analysis with large signal excitation, large deflection effects (NLGEOM, ON) and stress stiffening effects (SSTIF, ON) are enabled in transient analysis.

To simulate the operating condition, first, the dc bias voltage and the atmospheric pressure are applied on all elements in the model. Second, a short pulse from a zero-impedance voltage source is applied on the active element, while other elements have an open-circuit termination. For example, the short pulse is applied on two cells in the

TABLE II. CALCULATED PERFORMANCE OF THE DEVICES DESCRIBED IN TABLE I.

	Conventional CMUT	Collapse-mode CMUT
Peak frequency (MHz)	10.2	10.2
3-dB fractional bandwidth (%)	127.8	123.9
Output pressure sensitivity at 100 V dc (kPa/V)	13.1	46.5

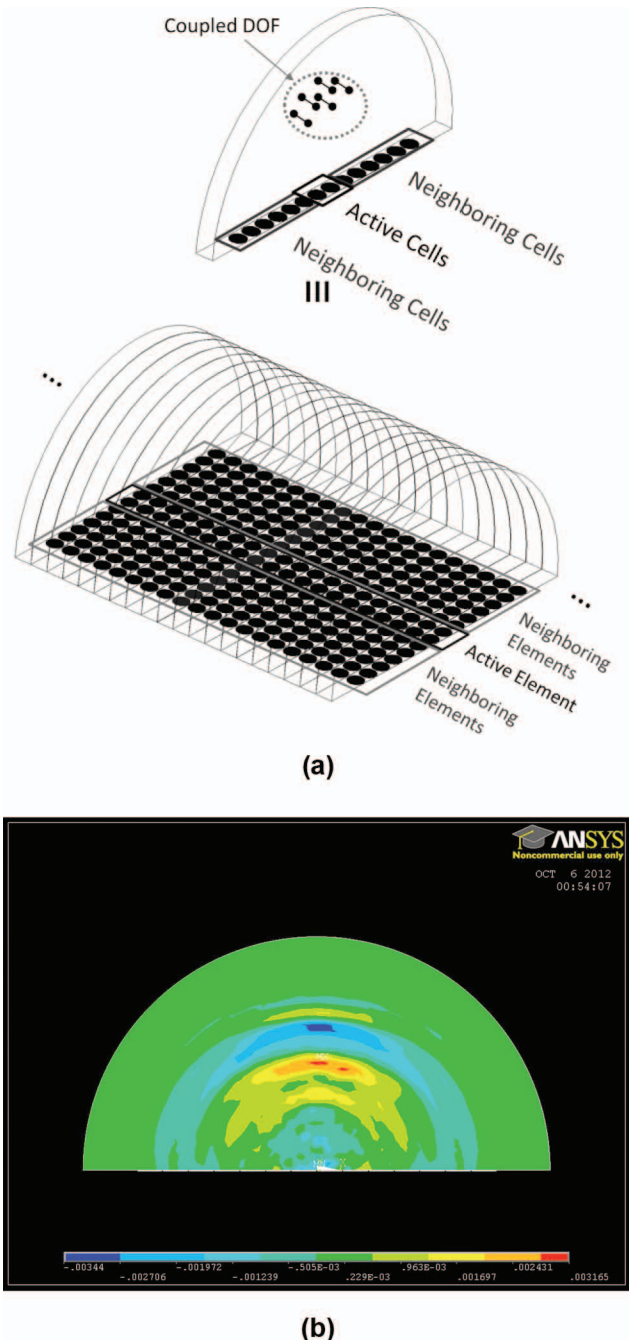


Fig. 4. (a) Diagram of the conventional CMUT in a 1-D linear array configuration. The FE model with 14 cells (shown on top) represents the CMUT array (shown at bottom). By coupling the degrees of freedom (DOFs) of the side of the medium, the FE model becomes equivalent to several CMUT elements of infinite length. (b) A snapshot of the 3-D FEA model for a 1-D array element. The contour represents the pressure in the medium.

center of the model in Fig. 4(b). After the excitation, a sound wave propagates through the medium as shown in Fig. 4(b). The pressure response is measured in the medium and the fast Fourier transform (FFT) was performed on the measured data to obtain the pressure frequency response. A 100 V dc bias and a 10 ns, 1 V unipolar excitation pulse was selected as input parameters. Fig. 5

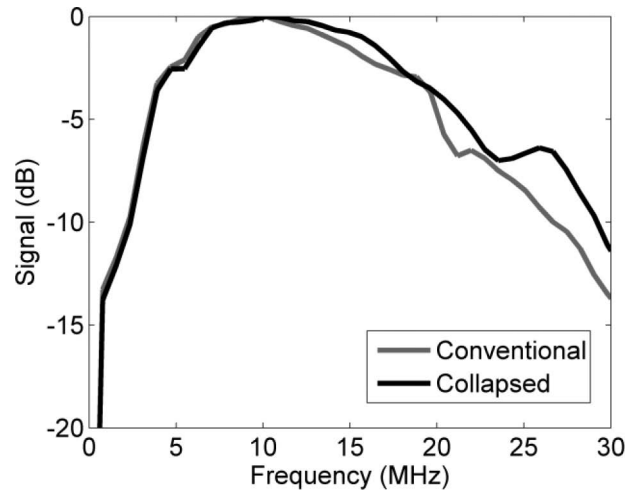


Fig. 5. The calculated frequency responses from the impulse responses of 3-D FEA models. The 3-dB FBW of the conventional CMUT and collapse-mode CMUT are 128% and 124%, respectively.

shows the calculated frequency response of the two devices in Table I. Because of the element-to-element interaction, the frequency response was not as smooth as the result presented in Fig. 2. The 3-dB FBWs of the conventional and the collapse-mode CMUTs are 128% and 124%, respectively, both centered at 10.2 MHz, which is similar to the results obtained using the 2-D FEA model.

The 2-D and 3-D FEA models showed that the designs presented in Table I meet the requirements in terms of the operating bias voltage and the center frequency. The FEA results suggest that the collapse-mode CMUT was superior to the conventional CMUT in terms of the output pressure and the FBW, when both devices have the same center frequency and the same plate thickness.

IV. DEVICE FABRICATION

To validate the FEA results and also to perform a fair comparison between the conventional and the collapse-mode CMUTs, the two devices described in Table I were fabricated. We chose to fabricate both devices on the same wafer, i.e., both devices have the same plate thickness. The additional gain of this approach was the elimination of any wafer-to-wafer variations. However, the two devices as shown in Table I have different gap heights. To realize two gap heights (250 and 500 nm) in a single wafer, we chose the LOCOS/wafer bonding process [11].

In the LOCOS/wafer bonding process, a highly conductive silicon plate is fusion bonded on pre-defined cavities; the radius and the depth of the cavity determines the radius of the plate and the gap height of the cell, respectively. The gap height was determined by the local oxidation of silicon, as shown in Fig. 6(a). The benefit of this fabrication process is that a cell with a reduced gap height could be designed by locating a predefined silicon step inside the cavity [Fig. 6(b)]. To achieve two different

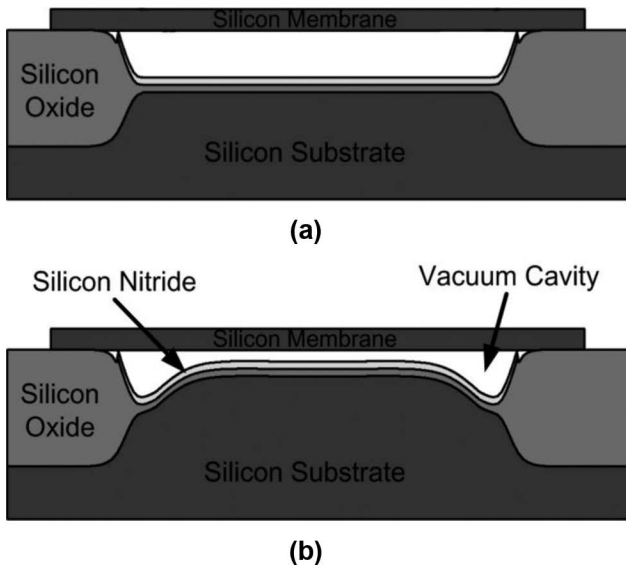


Fig. 6. Cross-sectional schematic of the unit cell of the CMUT. (a) The CMUT cell without the silicon step and (b) the cell with the silicon step inside the cavity. The LOCOS/wafer-bonding process enables fabrication of two different gap heights by introducing the silicon step inside the cavity.

gap heights (250 nm and 500 nm), we selected the height of the silicon step to be 250 nm [Fig. 6(b)] and the height of the gap resulting from the LOCOS process in Fig. 6(a) to be 500 nm. As insulation layers, 90-nm stoichiometric silicon nitride and 50-nm thermal oxide layers were used.

The two designs described in Table I were fabricated as shown in Fig. 7. The conventional CMUT had an element made of 156 cells in two columns [Fig. 6(a)], whereas the collapse-mode CMUT had an element made of 40 cells in a single column. Both devices had an element length of $2600\ \mu\text{m}$ and an element-to-element pitch of $75\ \mu\text{m}$ for a 10-MHz phased array configuration. The size of the 64-element array is $4800 \times 2600\ \mu\text{m}$. All cells in each element were connected electrically in parallel; for better electrical conductivity along the length of the element, thin aluminum metal lines were defined on the elements.

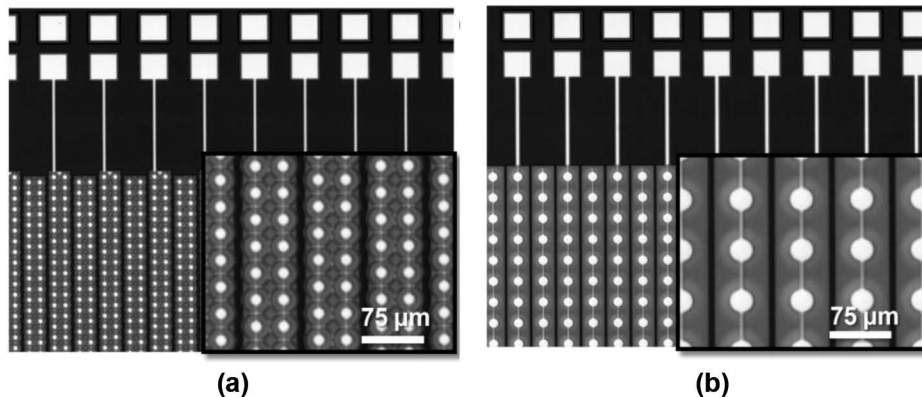


Fig. 7. Optical pictures of (a) the conventional CMUT and (b) the collapse-mode CMUT. Both devices have an element-to-element pitch of $75\ \mu\text{m}$ for 1-D phased array applications.

V. EXPERIMENTAL WORK

A. Frequency Response

To extract the frequency response of the two devices, we measured their transmit impulse response. The two devices were immersed in vegetable oil and a single element in the device was biased at 100 V and excited by a 10-V, 27-ns unipolar pulse by an arbitrary waveform generator (Model 33250A, Agilent Technologies Inc., Santa Clara, CA). In all measurements, the center elements in the array were used. During the measurement, neighboring elements were biased, but not excited by a pulse. The source impedances of the dc bias voltage and the pulse excitation were $1\ \text{M}\Omega$ (bias-T) and $50\ \Omega$, respectively. The displacement of the thin plate over several cells was measured using a laser Doppler vibrometer (LDV; OFV-511, Polytec GmbH, Waldbronn, Germany). The area scanning of the LDV validated the operating modes of the two devices, as shown in Fig. 8; the conventional device has the peak displacement at the center of the thin circular plate, whereas only the doughnut-shaped area moves in the collapse-mode device [Fig. 8(b)]. The acoustic impulse response was acquired by a calibrated hydrophone (HNP-0400, Onda Corp., Sunnyvale, CA), which was placed at a 6 mm distance on the central axis of the excited element [Figs. 9(a) and 9(b)]. Frequency responses of the two devices were obtained by computing the FFT of the received signal and including the correction for the input pulse spectrum and the sensitivity of the hydrophone [Fig. 9(c)]. The results from the measurements are summarized in Table III (see Table II for comparison).

B. Output Pressure

The output pressure is another key parameter for ultrasonic transducers. The output pressure was measured with various combinations of dc and ac voltages. The configuration of the electric excitation was identical to the one used in the previous section, except that a tone-

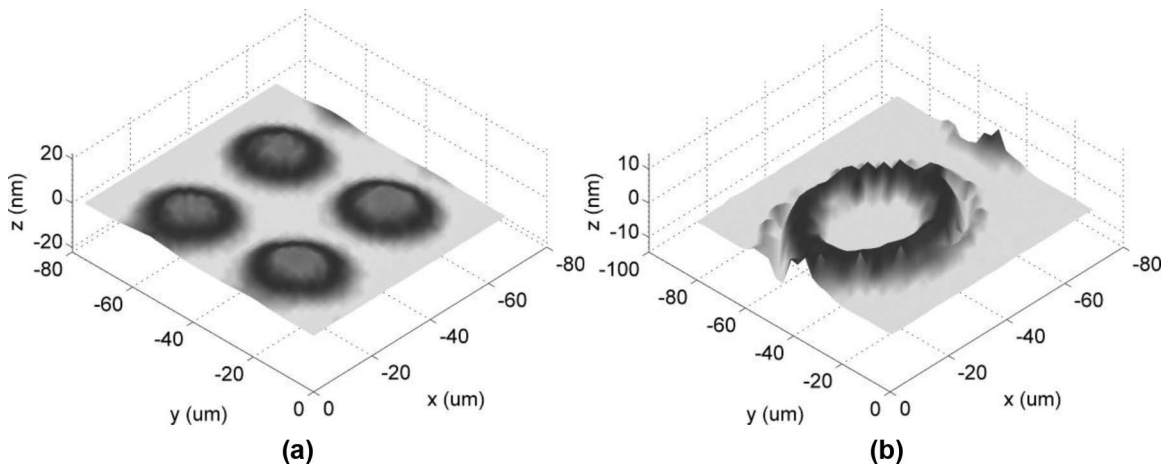


Fig. 8. Snapshots of displacement profiles of (a) the conventional CMUT and (b) the collapse-mode CMUT. These cells are located at the center of the measured elements. The collapse-mode CMUT presents an asymmetrical mode of vibration due to fabrication misalignments.

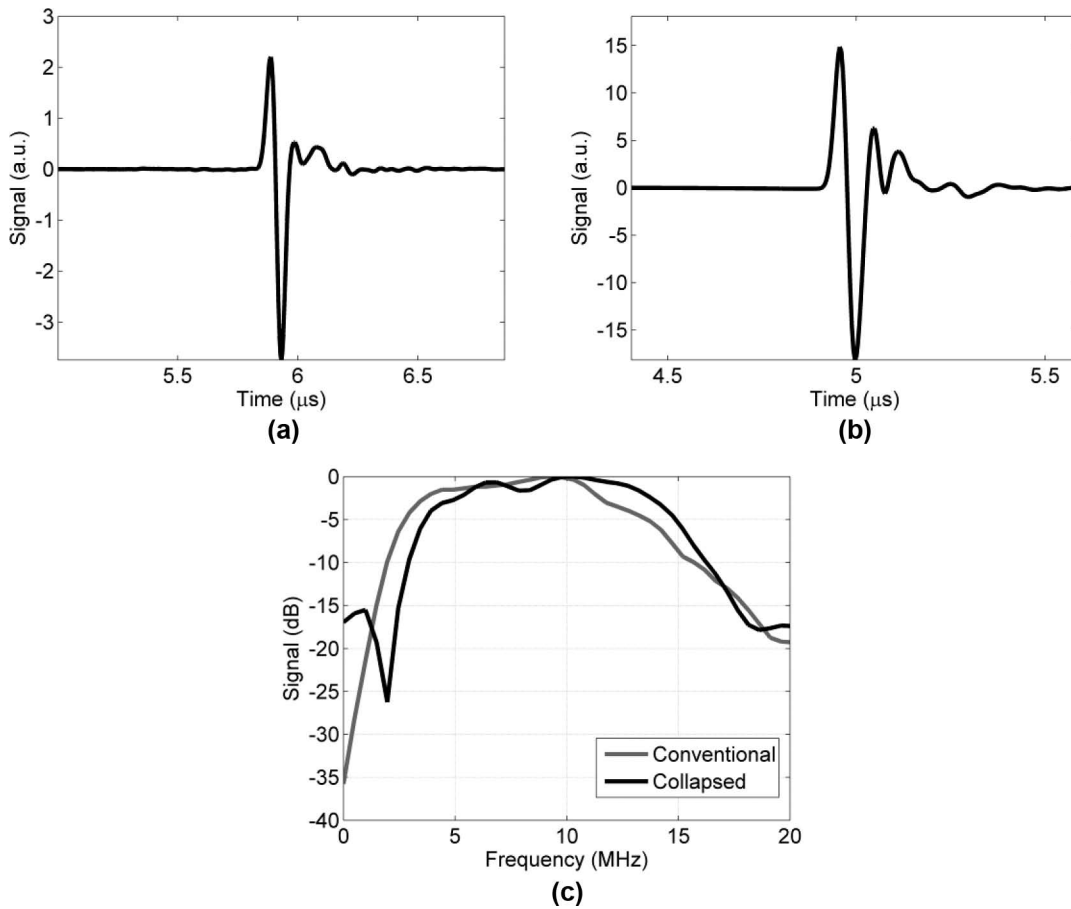


Fig. 9. (a) Impulse response of the conventional CMUT and (b) the collapse-mode CMUT, and (c) frequency response of the conventional and collapse-mode CMUTs. The response is measured using a calibrated hydrophone.

TABLE III. MEASURED PERFORMANCES OF FABRICATED DEVICES.

	Conventional CMUT	Collapse-mode CMUT
Peak frequency (MHz)	9.3	10.3
3-dB fractional bandwidth (%)	110.6	102.5
Output pressure sensitivity at 100 V dc (kPa/V)	12.7	26.4

burst signal was generated by RF power amplifier (Model 403LA, E&I Ltd., Rochester, NY) and the arbitrary waveform generator. A 10-MHz tone-burst signal with 10 cycles was applied to remove the interference from a reflected signal from the oil–air interface. The acoustic signal was then measured by a calibrated hydrophone located at a 6 mm distance on the central axis of the transducer array element. The received signal was converted into the output pressure of the transducer based on the sensitivity of the hydrophone, and corrected for the attenuation loss of the medium and the diffraction loss for the described geometry.

To measure the transmit sensitivity, the output pressure was measured with an ac input superimposed on various dc bias voltages ranging from 10 to 150 V. The measured output pressure per unit input ac voltage was compared with the results of the 2-D FE analysis, as shown in Fig. 10. The measured pressure of the conventional CMUT [Fig. 10(a)] is in good agreement with the FEA results up to the pull-in voltage (130 V). Both in the experiment and the FEA, the maximum output pressure sensitivity is measured as 18 kPa/V at 120 V. For the collapse-mode CMUT, a rapid increase of the output pressure after the pull-in voltage (70 V) is observed and the device showed maximum output pressure sensitivity of 40 kPa/V at 130 V. At the designed operating bias voltage, 100 V, the collapse-mode CMUT has higher output pressure than the conventional CMUT by factor of 1.8, which is, however, smaller than the factor of 3.5 from the FEA results.

In the collapse mode, the locations of the local maximum and minimum of the pressure are different between the FEA and the measurement; the FEA has the maximum at 110 V and the minimum at 130 V, whereas the measurement has the local maximum at 130 V and the local minimum at 150 V or more. In the collapse mode, the pressure peaks at a certain dc bias voltage because of the trade-off between the size of the ring-shaped moving area and the electric field intensity. When the bias voltage increases, the moving area is actuated by a higher electric

field, but the moving area becomes smaller and the center frequency of the moving area shifts away from the operating frequency.

There are two possible explanations for the discrepancies of the pressure and the dc bias voltage resulting in the maximum pressure: 1) the measurement presents the response of many plates, which have cell-to-cell variations, and 2) there are misalignments in the fabricated devices, as previously explained. Fig. 10 shows that the collapse-mode CMUTs are more sensitive to those effects.

To estimate the maximum output pressure, several ac and dc combinations were applied on the device, as shown in Fig. 11. The output pressure with a large ac input also showed that the collapse-mode CMUT had higher output pressure than the conventional CMUT; With a 28 V ac input, the maximum output pressure of the conventional CMUT and the collapse-mode CMUT were 443 kPa (at 120 V) and 1.19 MPa (at 120 V), respectively.

C. Linearity

Linearity is another important characteristic of an ultrasound transducer. In medical applications, second harmonic imaging (SHI) is now an indispensable function [13], which requires a broadband and linear transducer. In therapeutic ultrasound applications, such as HIFU, the second harmonic should be minimized to reduce heat generation in the interface between the body and the transducer.

To compare the linearity of the two devices experimentally, the output pressures of the two devices were measured using a calibrated hydrophone. Both devices were biased at 100 V, and excited using a 10-MHz 10-cycle tone burst signal. The second harmonic distortion (SHD) was extracted from the pressure measured in response to excitations with various ac input voltages.

The SHD analysis was performed in FEA for comparison. A temporal transient analysis was performed on the FEA model, which was described in Section III-A. Both

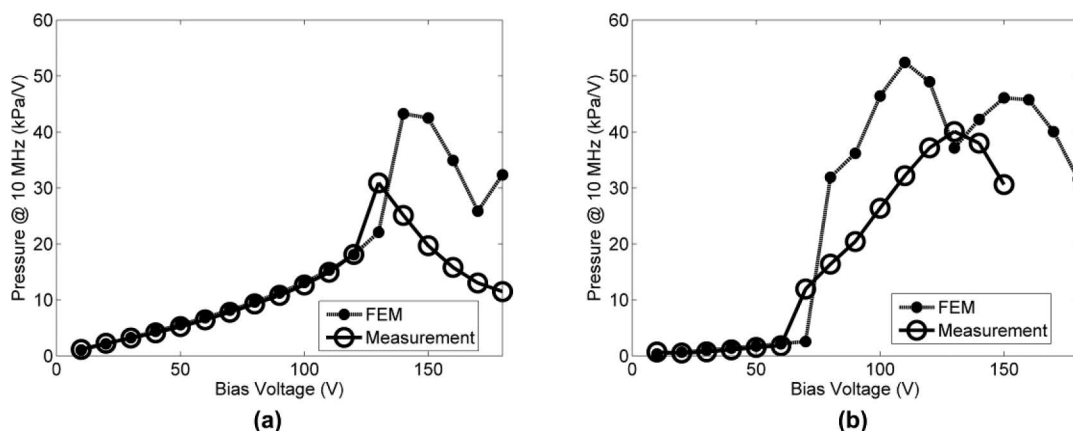


Fig. 10. The comparison of output pressure sensitivities of the FEA and the measurements: (a) for the conventional CMUT; (b) for the collapse-mode CMUT.

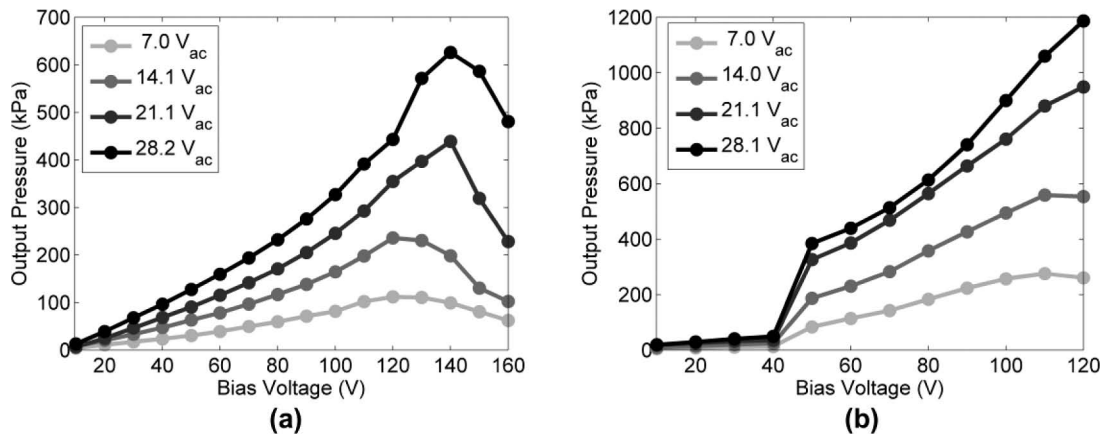


Fig. 11. The measured output pressure of (a) the conventional CMUT and (b) the collapse-mode CMUT in various ac and dc combinations.

the conventional and collapse-mode CMUT were biased at 100 V and excited by 10-MHz, 10-cycle, tone burst signals with various amplitudes. The SHD was extracted from the average pressure on top of the CMUT.

The comparisons between the conventional and collapsed-mode CMUT in the measurement and FEA are presented in Fig. 12. It turns out that the high transmit efficiency of the collapse-mode CMUT (shown in Fig. 11) is achieved at the expense of a high SHD. At the same transmit conditions, the collapse-mode CMUT presents a 5 dB higher SHD than the conventional SHD in the FEA. In the experimental results, the collapse-mode CMUT has a 10 dB higher SHD than the FEA results at most.

D. Long-Term Reliability

The charging effects of CMUTs have been observed in several cases. In the case of the CMUTs fabricated by the sacrificial release process [14], the plate was made of a dielectric material, which inherently trapped charges dur-

ing operation. Even in the case of the CMUTs based on the wafer bonding process, in which the plate was made of silicon, the insulation layer inside the cavity trapped charges [15]. The CMUT in the collapse-mode operation requires bias voltages higher than the pull-in voltage; the gap and the insulation layer will sustain high electric field intensity. Therefore, quantifying the effect of charging of the collapse-mode CMUT is of great interest.

To test the conventional and collapse-mode CMUTs at the same condition, both devices were biased at 100 V dc and a 30-V, 10-MHz, 30-cycle tone burst excitation was applied every 1 ms. The output pressure was continuously measured during this test (Fig. 13). After a short stabilization time of 30 min, the collapse-mode CMUT generated $634 \text{ kPa} \pm 15 \text{ kPa}$ continuously during 30 h of test. The total number of tone burst excitations during the operation was 3.2×10^9 cycles. Even though the collapse-mode CMUT had a much higher electric field inside the gap, the long-term stability of the device was comparable to that of the conventional CMUT.

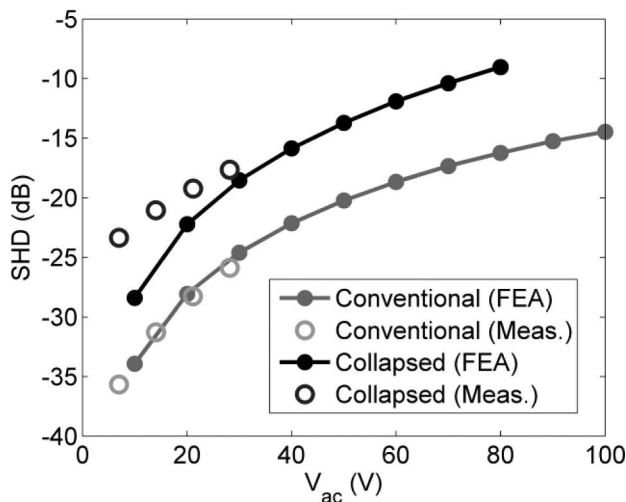


Fig. 12. Second harmonic distortion (SHD) of the two CMUTs (both at 100-V bias) extracted from the FEA results and the experimental measurements.

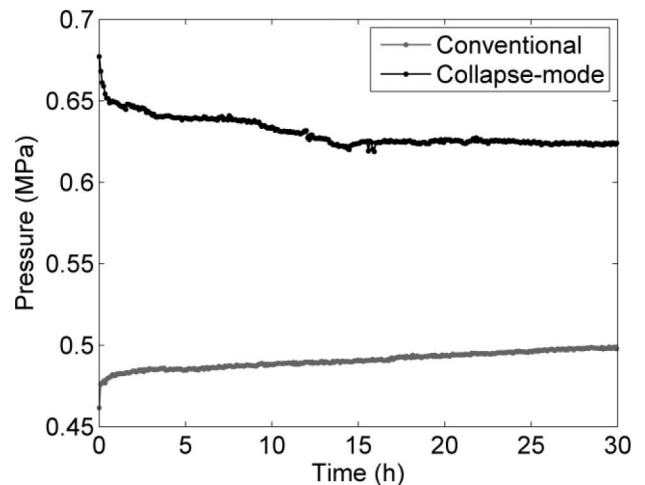


Fig. 13. Results of long-term stability test of two CMUTs biased at 100 V. A 30-cycle tone burst signal (10 MHz, 30 V ac) was applied on every 1 ms.

VI. DISCUSSION

The measurement of the output pressure and SHD of the conventional CMUT agreed well with the results from FEA, as shown in Fig. 10(a) and Fig. 12. However, the measured pressure of the collapse-mode CMUT at bias voltages ranging from 80 to 120 V [Fig. 10(b)] was lower than the FEA results by factor of 51% to 76%, as shown in Fig. 10(b). This is partially due to the asymmetry in the displacement profile of the collapse-mode CMUT plate. In ideal cases, the mode shape of the plate should be axisymmetric, whereas the measured results [Fig. 8(b)] presented an asymmetrical mode. This unwanted mode was mainly due to an alignment error between concentric structures, i.e., the cavity and the circular metal pad on the plate, during fabrication. Therefore, to maximize the performance of the collapse-mode CMUT, one must consider the effect of misalignment on the mode shape of the plate. Possible solutions are removing the metal pads on the plate or increasing the coverage of the metal to cover the whole cavity area. It should be also noted that the fabricated collapse-mode CMUT presented a performance in both output pressure and SHD level lower than what was predicted by the FEA model; this discrepancy was not observed in the conventional CMUT. Considering the fact that both devices were fabricated in the same wafer, the collapse-mode CMUT is more sensitive to practical device issues, such as misalignment and the friction force between the plate and the bottom electrode.

The high SHD level might limit some applications of the collapse-mode CMUT. For example, tissue harmonic imaging (THI) generally requires a level of SHD lower than -30 dB [16], [17], which cannot be fulfilled by the collapse-mode CMUT, when a sinusoidal signal is used for the excitation. However, once the nonlinearity of the CMUT is characterized, the high SHD of the collapse-mode CMUT can be improved by shaping the excitation signal. A 20-dB SHD reduction of a conventional CMUT was presented by Novell *et al.* [18] and the method can be applied to the collapse-mode CMUT.

In the case of the collapse-mode CMUT, the fabrication process affects the operating condition and the reliability. For example, the devices presented in this paper are based on a conductive plate, and therefore only 90-nm stoichiometric silicon nitride and 50-nm thermal oxide insulation layer should stand the high electric field in the contact area. The breakdown voltage highly depends on the combination of the dc bias and ac excitation. The insulation layer withstood 180 V dc, but broke down at 130 V dc bias combined with 30 V ac input. This breakdown condition limited the maximum output pressure of the collapse-mode CMUT. To improve the output pressure, one can increase the thickness of the insulation layers; however, it will introduce more charging effects, as shown by Huang [15]. Charging could lower the breakdown voltage of the device and could also affect its short-term stability. The rapid change in the output pressure we observed during the first 30 min of operation of a fresh device (Fig. 13)

is most probably due to charging in the dielectric layers under the cavity. Therefore, the thickness of the insulation layers should be minimized based on the optimal operating condition of the collapse-mode.

The work in this paper is based on the CMUTs fabricated by the wafer-bonding technique. Compared with the CMUTs based on the sacrificial release technique, the wafer-bonding CMUTs have several benefits in terms of the surface roughness of the bottom of the cavity and the uniformity of the plate thickness and the gap height. Because of the good controllability of dimensions, repeatable operation of the collapse mode was achieved in this work. CMUTs with a dielectric plate made using the sacrificial release process have different issues in operation. The plate acts as an insulation layer, and thus tolerates higher operating voltages in both ac and dc. However, the charging, and hence the long-term reliability, is a more severe issue in these devices. Therefore, a comparison between the conventional and collapse-mode CMUTs with dielectric plates would be an interesting and useful study.

VII. CONCLUSION

In this paper, we presented a comprehensive comparison between a conventional mode CMUT and a collapse-mode CMUT, each designed to operate at 10 MHz in their respective operating modes. The collapse-mode CMUT had better output pressure sensitivity over the conventional mode CMUT by a factor of 1.8 in spite of the existence of the asymmetrical mode. Even though the mode of operation was not ideal, the measured output pressure of the collapse-mode CMUT reached 1.19 MPa, which was much higher than that of the conventional CMUT (443 kPa). Another advantage of the collapse-mode operation is wide bandwidth exceeding 100% in a 1-D phased array configuration, which is comparable to that of the conventional CMUT. The high output pressure without sacrificing FBW is a key requirement for the collapse-mode CMUT as a future technology to be used in various applications. We believe that CMUTs, specifically designed and fabricated for the collapse-mode operation, can be another potential device that will be translated into successful practical use.

REFERENCES

- [1] X. C. Jin, F. L. Degertekin, S. Calmes, X. J. Zhang, I. Ladabaum, and B. T. Khuri-Yakub, "Micromachined capacitive transducer arrays for medical ultrasound imaging," in *Proc. IEEE Ultrasonics Symp.*, 1998, pp. 1877–1880.
- [2] Ö. Oralkan, A. S. Ergun, C.-H. Cheng, J. A. Johnson, M. Karaman, T. H. Lee, and B. T. Khuri-Yakub, "Volumetric ultrasound imaging using 2-D CMUT arrays," *IEEE Trans. Ultrason. Ferroelectr. Freq. Control*, vol. 50, no. 11, pp. 1581–1594, 2003.
- [3] A. Nikoozadeh, Ö. Oralkan, M. Gencel, J. W. Choe, D. N. Stephens, A. de la Rama, P. Chen, F. Lin, A. Dentinger, D. Wildes, K. Thomenius, K. Shivkumar, A. Mahajan, C. H. Seo, M. O'Donnell, U. Truong, D. J. Sahn, and P. T. Khuri-Yakub, "Forward-looking

- intracardiac imaging catheters using fully integrated CMUT arrays," in *Proc. IEEE Ultrasonics Symp.*, 2010, vol. 2, pp. 770–773.
- [4] I. O. Wygant, N. S. Jamal, H. J. Lee, A. Nikoozadeh, Ö. Oralkan, M. Karaman, and B. T. Khuri-Yakub, "An integrated circuit with transmit beamforming flip-chip bonded to a 2-D CMUT array for 3-D ultrasound imaging," *IEEE Trans. Ultrason. Ferroelectr. Freq. Control*, vol. 56, no. 10, pp. 2145–2156, Oct. 2009.
- [5] Ö. Oralkan, B. Bayram, G. G. Yaralioglu, A. S. Ergun, M. Kupnik, D. T. Yeh, I. O. Wygant, and B. T. Khuri-Yakub, "Experimental characterization of collapse-mode CMUT operation," *IEEE Trans. Ultrason. Ferroelectr. Freq. Control*, vol. 53, no. 8, pp. 1513–1523, Aug. 2006.
- [6] Y. Huang, E. Haeggström, B. Bayram, X. Zhuang, A. S. Ergun, C.-H. Cheng, and B. T. Khuri-Yakub, "Comparison of conventional and collapsed region operation of capacitive micromachined ultrasonic transducers," *IEEE Trans. Ultrason. Ferroelectr. Freq. Control*, vol. 53, no. 10, pp. 1918–1933, Oct. 2006.
- [7] B. Bayram, G. G. Yaralioglu, M. Kupnik, A. S. Ergun, Ö. Oralkan, A. Nikoozadeh, and B. T. Khuri-Yakub, "Dynamic analysis of capacitive micromachined ultrasonic transducers," *IEEE Trans. Ultrason. Ferroelectr. Freq. Control*, vol. 52, no. 12, pp. 2270–2275, Dec. 2005.
- [8] B. Bayram, E. Hægström, G. G. Yaralioglu, and B. T. Khuri-Yakub, "A new regime for operating capacitive micromachined ultrasonic transducers," *IEEE Trans. Ultrason. Ferroelectr. Freq. Control*, vol. 50, no. 9, pp. 1184–1190, 2003.
- [9] G. G. Yaralioglu, B. Bayram, and B. T. Khuri-Yakub, "Finite element analysis of CMUTS: Conventional vs. collapse operation modes," in *Proc. IEEE Ultrasonics Symp.*, 2006, pp. 586–589.
- [10] S. Olcum, F. Y. Yamaner, A. Bozkurt, H. Köymen, and A. Atalar, "An equivalent circuit model for transmitting capacitive micromachined ultrasonic transducers in collapse mode," *IEEE Trans. Ultrason. Ferroelectr. Freq. Control*, vol. 58, no. 7, pp. 1468–1477, Jul. 2011.
- [11] K. K. Park, H. J. Lee, M. Kupnik, and B. T. Khuri-Yakub, "Fabrication of capacitive micromachined ultrasonic transducers via local oxidation and direct wafer bonding," *J. Microelectromech. Syst.*, vol. 20, no. 1, pp. 95–103, 2011.
- [12] G. G. Yaralioglu, S. Ergun, and B. T. Khuri-Yakub, "Finite-element analysis of capacitive micromachined ultrasonic transducers," *IEEE Trans. Ultrason. Ferroelectr. Freq. Control*, vol. 52, no. 12, pp. 2185–2198, 2005.
- [13] F. Tranquart, N. Grenier, and V. Eder, "Clinical use of ultrasound tissue harmonic imaging," *Ultrasound Med. Biol.*, vol. 25, no. 6, pp. 889–894, 1999.
- [14] S. Machida, S. Migitaka, H. Tanaka, K. Hashiba, H. Enomoto, Y. Tadaki, and T. Kobayashi, "Analysis of the charging problem in capacitive micro-machined ultrasonic transducers," in *Proc. IEEE Ultrasonics Symp.*, 2008, pp. 383–385.
- [15] Y. Huang, E. Haeggström, X. Zhuang, A. S. Ergun, and B. T. Khuri-Yakub, "A solution to the charging problems in capacitive micromachined ultrasonic transducers," *IEEE Trans. Ultrason. Ferroelectr. Freq. Control*, vol. 52, no. 4, pp. 578–580, 2005.
- [16] M. A. Averkiou, D. N. Roundhill, and J. E. Powers, "A new imaging technique based on the nonlinear properties of tissues," in *Proc. IEEE Ultrasonics Symp.*, 1997, pp. 1561–1566.
- [17] M. A. Averkiou, "Tissue harmonic imaging," in *Proc. IEEE Ultrasonics Symp.*, 2000, vol. 2, pp. 1563–1572.
- [18] A. Novell, M. Legros, N. Felix, and A. Bouakaz, "Exploitation of capacitive micromachined transducers for nonlinear ultrasound imaging," *IEEE Trans. Ultrason. Ferroelectr. Freq. Control*, vol. 56, no. 12, pp. 2733–2743, Dec. 2009.



Kwan Kyu Park (S'10–M'12) received the B.S. degree in mechanical and aerospace engineering from Seoul National University, Seoul, Korea, in 2001. He received the M.S. and Ph.D. degrees in mechanical engineering from Stanford University, Stanford, CA, in 2007 and in 2011, respectively. He has been a Research Assistant in the Edward L. Ginzton Laboratory, Stanford University, since 2006. His research interests include chemical/biological sensors based on micromechanical resonators, multi-resonator systems, charging of MEMS devices, ultrasonic transducers, and RF MEMS.



Ömer Oralkan (S'93–M'05–SM'10) received the B.S. degree from Bilkent University, Ankara, Turkey, in 1995; the M.S. degree from Clemson University, Clemson, SC, in 1997; and the Ph.D. degree from Stanford University, Stanford, CA, in 2004, all in electrical engineering. Dr. Oralkan was a Research Associate from 2004 to 2007 and then a Senior Research Associate from 2007 to 2011 in the Edward L. Ginzton Laboratory at Stanford University. He was an Adjunct Lecturer from 2009 to 2011 in the Department of Electrical Engineering at Santa Clara University, Santa Clara, CA. Currently, he is an Associate Professor of electrical and computer engineering at North Carolina State University, Raleigh, NC. His current research focuses on developing devices and systems for ultrasound imaging, photoacoustic imaging, image-guided therapy, biological and chemical sensing, and ultrasound neural stimulation. Dr. Oralkan authored more than 120 publications and received the 2002 Outstanding Paper Award of the IEEE Ultrasonics, Ferroelectrics, and Frequency Control Society. He is a Senior Member of the IEEE and serves on the Technical Program Committee of the IEEE Ultrasonics Symposium.



Butrus (Pierre) T. Khuri-Yakub is a Professor of electrical engineering at Stanford University. He received the B.S. degree from the American University of Beirut, the M.S. degree from Dartmouth College, and the Ph.D. degree from Stanford University, all in electrical engineering. His current research interests include medical ultrasound imaging and therapy, chemical/biological sensors, micromachined ultrasonic transducers, and ultrasonic fluid ejectors. He has authored more than 500 publications and has been principal inventor or co-inventor of 92 US and internationally issued patents. He was awarded the Medal of the City of Bordeaux in 1983 for his contributions to nondestructive evaluation, the Distinguished Advisor Award of the School of Engineering at Stanford University in 1987, the Distinguished Lecturer Award of the IEEE UFFC society in 1999, a Stanford University Outstanding Inventor Award in 2004, the Distinguished Alumnus Award of the School of Engineering of the American University of Beirut in 2005, the Stanford Biodesign Certificate of Appreciation for commitment to educate, mentor and inspire Biodesign Fellows in 2011, and is the 2011 recipient of the IEEE Rayleigh award.